Catalysis Science & Technology

Accepted Manuscript

ROYAL SOCIETY OF CHEMISTRY

www.rsc.org/catalysis

Journal Name

ARTICLE

Comparative study of silica-supported copper catalysts prepared by different methods: Formation and transition of copper phyllosilicate

Received 00th January 20xx,
Accepted 00th January 20xx

DOI: 10.1039/x0xx00000x

www.rsc.org/

Xiaohuan Dong,[a,b] Xiangang Ma,[a,*] Hengyong Xu[a] and Qingjie Ge[a,*]

Cu/SiO_2 catalysts prepared by ion exchange (IE), deposition precipitation (DP), homogeneous deposition-precipitation (HDP) using urea hydrolysis and ammonia evaporation method (AE) were systematically characterized focusing on the formation and transition of copper phyllosilicate. It generated during the AE, IE and HDP methods and decomposed to CuO after the calcination at 450 °C, which was supported by BET, TPR, XRD and TEM. Copper phyllosilicate can be reduced to Cu^0 rather than Cu^+ below 350 °C. The formation of copper phyllosilicate promoted the dispersion of copper species. The Cu/SiO_2 catalyst prepared by the AE method possessed the highest Cu^0 dispersion due to the high content of copper phyllosilicate in the catalyst precursor and thus exhibited the best activity for the hydrogenation of methyl acetate.

Introduction

Hydrogenation of esters to the corresponding alcohols is a fundamental reaction in organic chemistry and is employed in a large number of chemical processes. Of particular interest are the hydrogenation of acetic esters to the promising fuel ethanol and the hydrogenation of diesters to diols which are used in the production of polyesters. Silica-supported copper catalysts have been identified as the promising catalysts for these reactions and many maneuverable methods such as impregnation (IM)[1,2], ion exchange (IE) with tetrammine copper cations[3,4] , deposition-precipitation (DP) method[5,6], homogeneous deposition-precipitation (HDP) assisted by the hydrolysis of urea[7-9] and ammonia evaporation (AE) method[10-12] were studied extensively in order to develop a better catalyst. The Cu/SiO_2 catalyst prepared by the AE method exhibited high activity and stability for ester hydrogenation and thus AE method drew much attention in recent years. It is believed that the formation of copper phyllosilicate in AE method, also called chrysocolla, was important for the outstanding catalytic performance of Cu/SiO_2 catalyst. Chen et al.[10] proposed a cooperative effect of Cu^0 and Cu^+ in ester hydrogenation and attributed Cu^0 and Cu^+ to the reduction of highly dispersed CuO and copper phyllosilicate respectively, which was supported by Yue et al.[13-15] and Li et al.[16] In contrast, Yuan's group reported that the reduction of copper phyllosilicate yielded Cu nanoparticles and the increase of copper phyllosilicate content boosted the dispersion of Cu^0 and the activity of the catalyst.[17,18] In addition, Cu^+ widely existed in the chrysocolla-absent catalysts.[2,5,19] Whether copper phyllosilicate is the source of Cu^+ or not is still in dispute.

In the present work, Cu/SiO_2 catalysts were prepared by the IE, DP, HDP and AE methods and systematically characterized using ICP, BET, TPR, XRD, TEM and N_2O-oxidation to discuss the formation and transition of copper phyllosilicate. The catalytic performance of the Cu/SiO_2 catalysts was evaluated using the hydrogenation of methyl acetate (MA) as the probe reaction and correlated with the characterization results to reveal why AE method is a suitable means to prepare high-performance Cu/SiO_2 catalyst for ester hydrogenation.

Experimental

Catalyst preparation

Cu/SiO_2 catalysts were prepared by four methods, namely the ammonia evaporation method (AE), ion exchange method (IE), deposition precipitation method (DP) and homogeneous deposition precipitation assisted by urea hydrolysis (HDP). The corresponding catalysts were denoted as AECu, IECu, DPCu, and HDPCu, respectively. The nominal Cu loading of the four catalysts was 20%.

For the AECu method, 11.3 g of $Cu(NO_3)_2{\cdot}3H_2O$ (Tianjin Kermel Corp) was dissolved in 150 ml of deionized water and 18 ml of 28% ammonia aqueous solution (Tianjin Kermel Corp) was added within 30 min under agitation. Then, 12.0 g of SiO_2 (Evonik Degussa) was added into the formed copper ammonia complex solution. The initial pH of the suspension was ca. 9. After stirred for 4 h at 35 °C, the temperature was increased to 90 °C to allow for the evaporation of ammonia and the

[a] Dalian National Laboratory for Clean Energy, Dalian Institute of Chemical Physics, Chinese Academy of Sciences, Dalian 116023, Liaoning, China. E-mail: xiangangma@dicp.ac.cn, geqj@dicp.ac.cn; Fax: +86 411 84379152; Tel: +86 411 84379229.
[b] University of Chinese Academy of Sciences, Beijing 100039, China.

deposition of copper species onto the silica. When the pH value of the suspension decreased to 6-7, the evaporation procedure was terminated and this step required about 2 h. The filtrate was washed with deionized water and dried overnight at 120 ^{o}C.

For the IECu method, 11.3 g of $Cu(NO_3)_2{\cdot}3H_2O$ was dissolved in 150 ml of deionized water and ammonia aqueous solution was applied to adjust the pH value to 11-12. Then 12.0 g of SiO_2 was added and stirred for 12 h at room temperature. The mixture was filtered and washed with deionized water and then the sample was dried at 120 ^{o}C overnight.

For the DPCu method, 11.3 g of $Cu(NO_3)_2{\cdot}3H_2O$ was dissolved in 150 ml of deionized water at room temperature and 12.0 g of SiO_2 was added to form a suspension. Subsequently, 37 ml of 28% ammonia aqueous solution was added dropwise into the suspension to precipitate the copper species to the support. The final pH value was 7-8. After aging for 2 h, the mixture was filtered and washed with deionized water and then the sample was dried at 120 ^{o}C overnight.

For the HDPCu method, 11.3 g of $Cu(NO_3)_2{\cdot}3H_2O$ and 28.2 g of urea were dissolved in 150 ml of deionized water at room temperature and 12.0 g of SiO_2 was added to form a suspension under agitation. Then the solution was kept at 90 ^{o}C to hydrolyze the urea. When the pH value of the suspension reached 6-7, the heating process was terminated. The mixture was filtered and washed with deionized water and then the sample was dried at 120 ^{o}C overnight.

Before the reaction of methyl acetate hydrogenation, the catalyst samples were calcined at 450 ^{o}C for 4 h, pelletized, crushed and sieved to 20-40 meshes.

Catalyst characterization

The copper loading was determined by the inductively coupled plasma atomic emission spectroscopy (ICP-AES). Nitrogen adsorption-desorption isotherms were measured by static N_2 adsorption at -196 ^{o}C with a Quantachrome NOVA4000 analyzer. Before the N_2 physisorption measurement, all the samples were outgassed at 120 ^{o}C for 1 h and then evacuated at 300 ^{o}C for 3 h to remove physically adsorbed impurities. The specific surface area was calculated by the Brunauer–Emmett–Teller (BET) method. The total pore volume (Vp) was derived from the adsorbed N_2 volume at a relative pressure of approximately 0.98, and the Barrett–Joyner–Halenda (BJH) method was applied to calculate the pore size distributions according to the desorption branch of the isotherms.

Temperature-programmed reduction (TPR) was carried out on a home-made apparatus. 40 mg of the Cu/SiO_2 sample was outgassed at 120 ^{o}C under Ar for 1 h. After cooling to room temperature, the gas was switched to 5% H_2-95% Ar, and the sample was heated to 950 ^{o}C at a ramping rate of 3.4 K/min. The amount of H_2 consumed was monitored by a thermal conductivity detector (TCD).

The copper surface areas and dispersions of the catalysts were determined on a Quantachrome Autosorb iQ2 instrument by the reduction/H_2-oxidation/N_2O-reduction/H_2 method.[12] Initially, 70 mg of the catalyst sample was reduced in 5% H_2-95% Ar at 350 ^{o}C for 3 h and cooled down to 90 ^{o}C. 10% N_2O-90 % He was passed through the catalyst bed for 1 h to completely oxidize surface copper atoms to Cu_2O. Then the formed Cu_2O was reduced at 350 ^{o}C and the amount of consumed H_2 was detected by TCD. Copper dispersion was calculated by dividing the amount of surface copper atom by the total number of supported copper atoms per gram of catalyst. The metallic copper surface area was computed based on an atomic copper surface density of 1.46×10^{19} Cu atoms/m^2.

XRD patterns were collected on an X´Pert PRO diffractometer (PANalytical). Ordinary XRD characterization was carried out with a Cu-Kα radiation of 40 kV and 40 mA and powder catalyst was used. For the reduced catalysts, helium was used to protect the reduced catalysts to avoid long time exposure to air. In-situ XRD was carried out with a Cu-Kα radiation of 40 kV and 300 mA. Catalyst sample was shaped into a plate with a diameter of 13 mm and a thickness of 1.5 mm before the characterization.

Transmission electron microscopy (TEM) images were obtained on a JEM-2100 transmission electron microscope operating at an acceleration voltage of 300 kV. To prepare an appropriate sample for TEM observation, catalyst powder was ultrasonically dispersed in ethanol at room temperature for 30 min and transferred onto carbon-coated copper or nickel grid by dipping. The average particle size was calculated using $d = \sum n_i d_i^3 / \sum n_i d_i^2$, where n_i is the number of particles having a characteristic diameter d_i.

Activity test

The catalytic performance of the catalyst was tested in a continuous-flow fixed-bed reactor. Typically, 1 g catalyst was packed into a stainless steel tubular reactor (internal diameter of 12 mm) with the thermocouple inserted into the catalyst bed. Before reaction, the catalyst was activated at 350 ^{o}C for 3 h in a pure hydrogen flow with a ramping rate of 1 ^{o}C/min. Methyl acetate was injected into the vaporizer, heated and then introduced into the reactor by H_2. The products were introduced in a gaseous state and analyzed on line by a Varian CP 3800 gas chromatograph with a flame ionization detector (FID).

Results

Physicochemcial properties of Cu/SiO_2 samples

The physicochemical properties of the Cu/SiO_2 samples are summarized in Table 1. For the IE method, the washing solution was deep blue-colored indicating the incomplete depletion of the copper species and the Cu loading was only 7.0%, much lower than the nominal number. For the AE and HDP method, the copper loading was slightly lower than the pre-set value . This was because parts of copper precursors still remained in the solution after the ammonia evaporation and urea hydrolyzation. The conventional DP method resulted in the decrease of BET surface area due to the coverage and aggregation of copper species on the surface of the SiO_2

support. The increase of BET surface area in the other three methods implied the generation of new surface area. This may be attributed to the formation of copper phyllosilicate which has a high specific surface area due to its special "plate-like" structure as reported in the published papers.[10,11]

The N_2 adsorption-desorption isotherms of the Cu/SiO_2 samples and their pore size distribution curves are illustrated in Fig. 1. Both the SiO_2 support and the catalyst samples exhibited Langmuir type IV isotherms, corresponding to a typical mesoporous material. The hysteresis loop tended to change from H1-type to H4-type after the introduction of copper species, and the pore shape from "spherical" to "slit-like". This change was prominent in the samples prepared by the AE and HDP methods. Copper phyllosilicate could be formed in this two methods. The original silica support will be consumed to form it. The structure of SiO_2 changed. For the AE method, two small pores emerged at ca. 3.7 nm and 5.8 nm in the dried sample and the latter moved to ca. 7.8 nm in the calcined sample, meanwhile the pores of the support between 10 nm and 28 nm disappeared. Accordingly, the average pore diameter and pore volume drastically reduced compared to the SiO_2 support. The HDP method gave similar trend to the AE method in pore size and volume. The difference was that the two small pores appeared at ca. 3.7 nm and 4.8 nm in the dried HDPCu sample. The pore size and volume of the IECu and DPCu samples also altered with the ablation of the large pores.

Table 1 Textural properties of Cu/SiO_2 samples

Samples	Cu loading[a]	S_{BET} ($m^2\ g^{-1}$)		V_p ($cm^3\ g^{-1}$)		D_p (nm)		S_{Cu}[b] ($m^2\ g^{-1}$)	D_{Cu}[c] (%)	d_{Cu}[d] (nm)	d_{Cu}[e] (nm)	d_{Cu}[f] (nm)
		dried	calcined	dried	calcined	dried	calcined					
SiO_2			203		0.90		17.66					
DPCu	20.1	144	150	0.55	0.57	15.17	15.08	6.09	4.7	21.8	>100	57
IECu	7.0	237	259	0.57	0.73	9.62	11.29	12.4	27.5	3.7	3.4	<3
AECu	17.0	358	350	0.45	0.52	5.0	5.92	41.4	37.8	2.7	5.2	3.5
HDPCu	18.9	281	322	0.33	0.55	4.72	6.81	18.3	15.0	6.8	5.8	4.5

a Determined by ICP-AES analysis.

b Cu metal surface area , c copper dispersion and d Cu metal particle size determined by the N_2O titration method.

e Determined by TEM.

f Cu crystallite size calculated by the Scherrer formula.

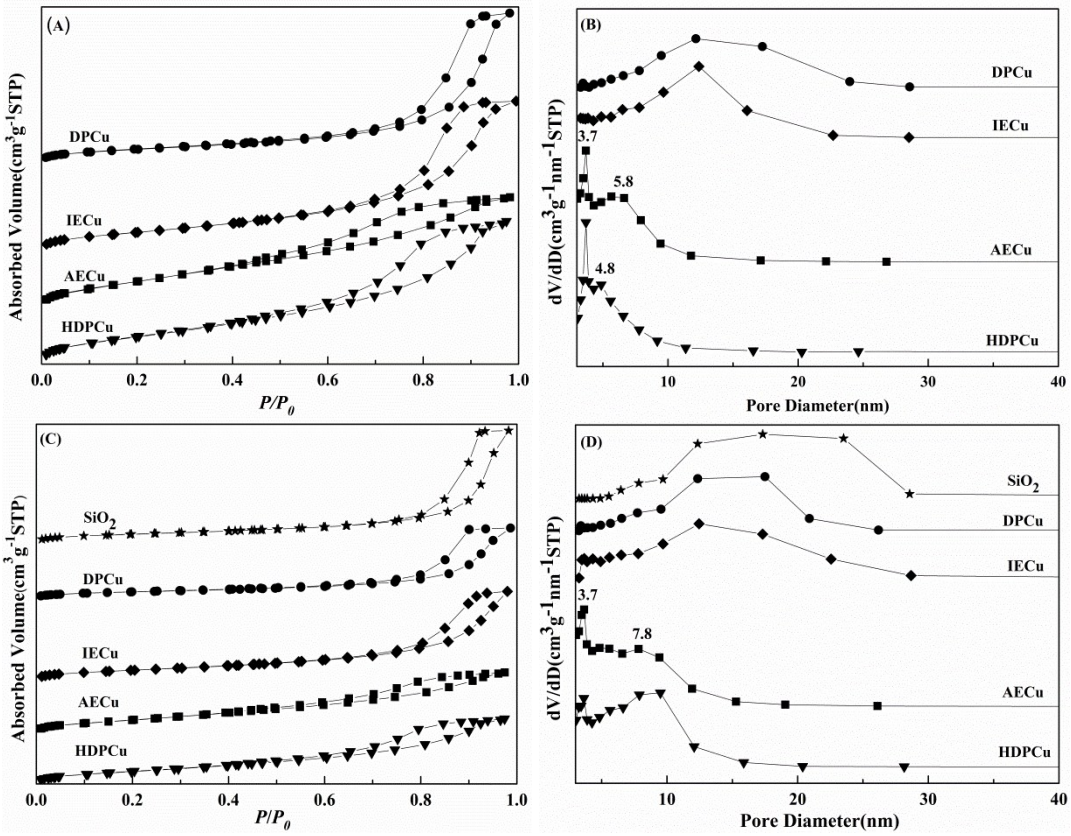

Fig. 1 N_2 adsorption-desorption isotherms and pore size distribution curves of the Cu/SiO_2 samples. (A) and (B) for the dried samples, (C) and (D) for the calcined samples.

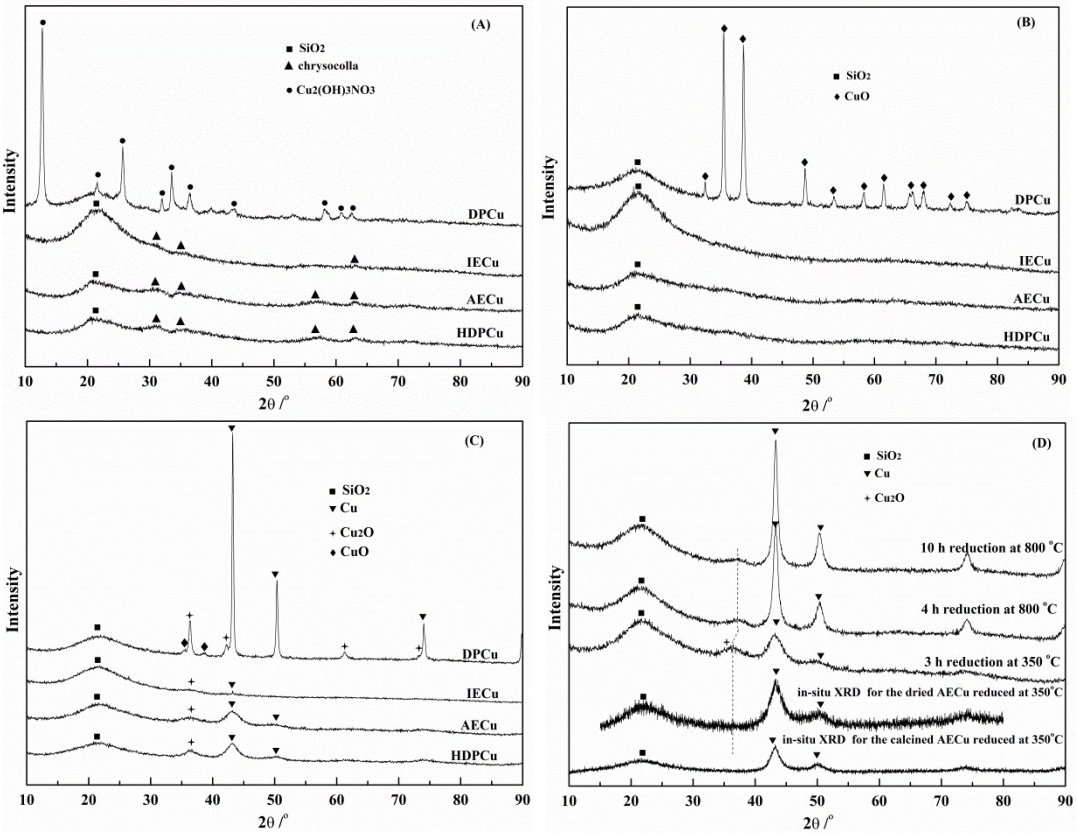

Fig. 2 XRD patterns of the Cu/SiO_2 samples. (A) dried, (B) calcined, (C) reduced, (D) AECu with different treatments and in-situ XRD

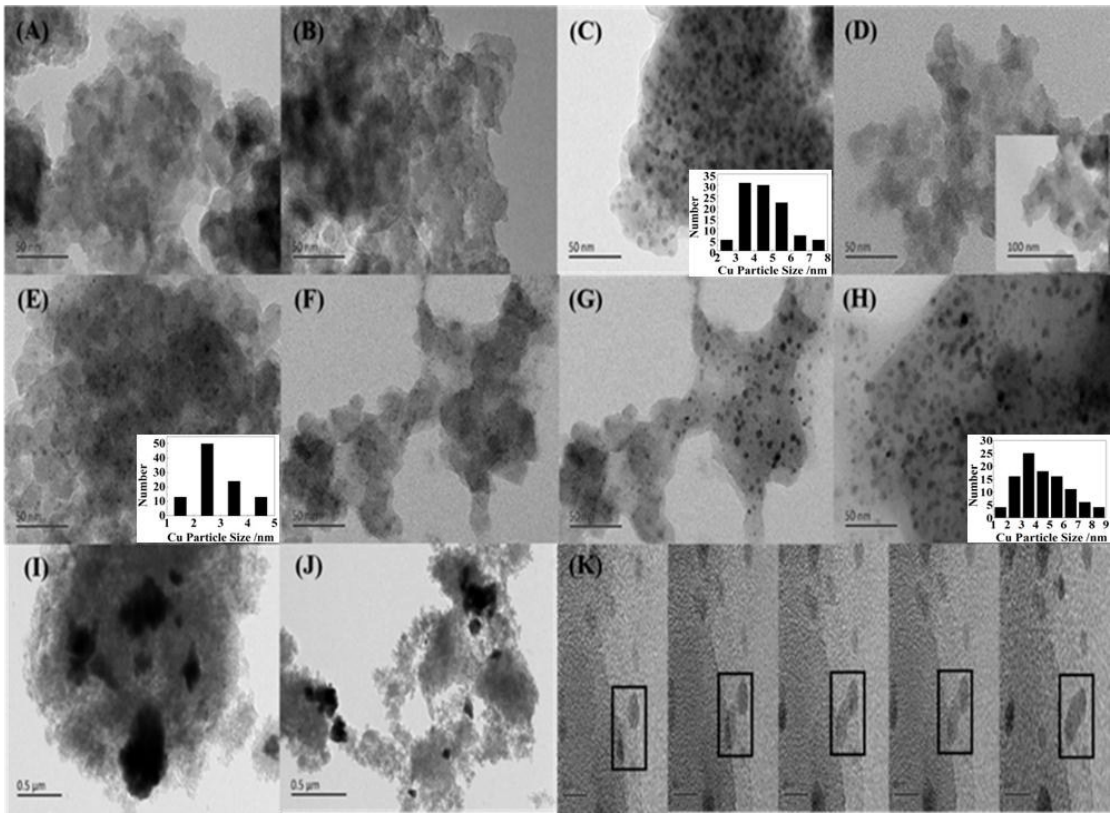

Fig. 3 TEM images of the Cu/SiO_2 samples. (A) dried AECu, (B) calcined AECu, (C) reduced AECu, (D) calcined IECu, (E) reduced IECu, (F) calcined HDPCu, (G) calcined HDPCu after 15 min exposure to the electron beam, (H) reduced HDPCu, (I) calcined DPCu, (J) reduced DPCu, (K) agglomeration of two particles in calcined HDPCu

XRD patterns of Cu/SiO_2 samples

XRD patterns of the Cu/SiO_2 samples are collected in Fig. 2. The peak at about $2\theta = 21.7^o$ belongs to amorphous silica. Copper species in the dried DPCu mainly existed in the form of cupric hydroxide nitrate (JCPDS 003-0061), and then transformed to copper oxide (JCPDS 005-0661) after the calcination. The broad diffraction peaks at 31.2^o, 35.8^o, 57.3^o and 63.2^o in the dried AECu and HDPCu suggested the presence of copper phyllosilicate[13,18] and the disappearance of these peaks indicated the decomposition of copper phyllosilicate to CuO at 450 °C. The formed CuO in the calcined AECu and HDPCu did not exhibit any diffraction peaks. After the reduction at 350 °C, the diffraction peaks for metallic copper appeared at 43.3^o, 50.4^o and 74.1^o (JCPDS 004-0836) in the reduced AECu and HDPCu. The copper particle size in these two catalysts was 3.5 nm and 4.5 nm, respectively. Meanwhile, another peak was observed at 36.5^o, which did not show up in the in-situ XRD characterization of the dried and calcined AECu reduced at 350°C (Fig. 2D).The highly dispersed metallic copper can be oxidized to Cu_2O or CuO to some extent when exposure to air. The final state may be determined by the particle size and the copper-support interaction. The peak at 36.5^o in the reduced AECu and HDPCu can be assigned to Cu_2O obtained from the oxidation of Cu^0 in air. Fig. 2D shows that heightening the reduction temperature and prolonging the reduction time resulted in the aggregation of the copper particles. The metal-support interaction decreased with the increase of the copper particle size. Compared to the reduction at 350 °C, the oxidation of Cu^0 became weaker after the reduction at 800 °C based on the peak area. In addition, some of the metallic copper tended to be oxidized to CuO other than Cu_2O due to the poorer metal-support interaction and this caused a slight shift of the oxidation peak towards the high-angle side. The interaction in the DPCu sample is weaker than the AECu and HDPCu samples. Some of Cu^0 in the reduced DPCu was oxidized to CuO showing diffraction peaks at 35.5^o and 38.7^o, and some of Cu^0 was oxidized to Cu_2O. However, the possibility that Cu_2O came from the incomplete reduction of the large CuO particles could not be excluded.

The peaks for copper phyllosilicate in the dried IECu were much weaker than the dried AECu and HDPCu. One reason for this was the low copper loading of 7.0%. Another reason was that some copper existed in other forms, for instance isolated copper ions and CuO. After the reduction, a weak peak of Cu appeared at 43.3^o. The tiny Cu_2O peak at 36.5^o can be attributed to the same source as the reduced AECu and HDPCu.

TEM images of Cu/SiO_2 samples

Fig. 3 shows the typical TEM images of the Cu/SiO_2 samples. Different from Zheng's[18] and Chen's[10] work, copper phyllosilicate did not exhibit a filandrous morphology in the present work (Fig. 3A). As shown in Fig. 3B, CuO was in a high dispersion in the calcined AECu and no black spot of CuO showed up in the TEM images. For the calcined IECu, the morphology in most regions was similar to the calcined AECu. However, small particles of CuO appeared in some areas (inset of Fig. 3D). Koler et al.[4] reported that for the IE method dissolved Cu^{2+} ions, present in the interstitial particle volumes, were precipitated as $Cu(OH)_2$ upon washing with distilled water and retained in the catalysts. The CuO particles in calcined IECu should come from the decomposition of this kind of $Cu(OH)_2$. For the calcined HDPCu, the observed CuO particles were sensitive to the electron beam. The CuO particles were small and not obvious at first (Fig. 3F), then became bigger due to the agglomeration (Fig. 3G) with the extension of the exposure time. Fig. 3K presented the agglomeration procedure of two small particles into a big one. Well-dispersed Cu particles appeared in the reduced catalysts in the order of $d_{HDPCu} > d_{AECu} > d_{IECu}$ with the average particle size of 5.8 nm, 5.2 nm and 3.4 nm, respectively. The average particle size was calculated based on the statistics of about 100 particles from the TEM images in different areas. As shown in the histograms of the particle size distribution at the right corner of the reduced IECu image, most of the Cu particles were in the range of 3-4nm and no particles larger than 5nm were detected. The intensity of the Cu^0 particles in the reduced IECu was much lower than the two others due to the low copper loading. For the calcined and reduced DPCu, large black CuO and Cu particles can be observed, suggesting a poor dispersion of copper species. The metallic Cu particle size observed by TEM is larger than the crystallite size derived from XRD, indicating the polycrystalline nature of the metallic Cu particles. The metallic Cu particle size calculated from N_2O chemisorption was similar to the TEM results for IECu and HDPCu but smaller than the TEM results for DPCu and AECu.

TPR profiles of Cu/SiO_2 samples

In the present work, TPR measurement was carried out from 25 to 950 °C for all the samples. For clarity, only the data below 500 °C were shown in Fig. 4 since no peak was observed above 500 °C. With the help of TPR and other techniques, Van Der Grift et al[20] proved the existence of copper phyllosilicate in the dried Cu/SiO_2 samples prepared by the HDP and IE methods using several mineral copper hydrosilicates as reference compounds including chrysocolla. In the present work, the dried samples except dried DPCu showed two reduction peaks similar to Van Der Grift's report, implying the presence of copper phyllosilicate. The calcined samples exhibited only one narrow and symmetric reduction peak, indicating the decomposition of copper phyllosilicate after the calcination, which was accordance with the TEM and XRD results. The reduction peak of the calcined IECu, AECu and HDPCu samples centered at 210-213 °C, much lower than the bulk CuO (263 °C) due to the higher surface area exposed to H_2 and the interaction between copper species and the support.[5] With the relatively larger and uneven particles, the calcined DPCu gave a broad and asymmetrical reduction peak centered at a little higher temperature of 227 °C.

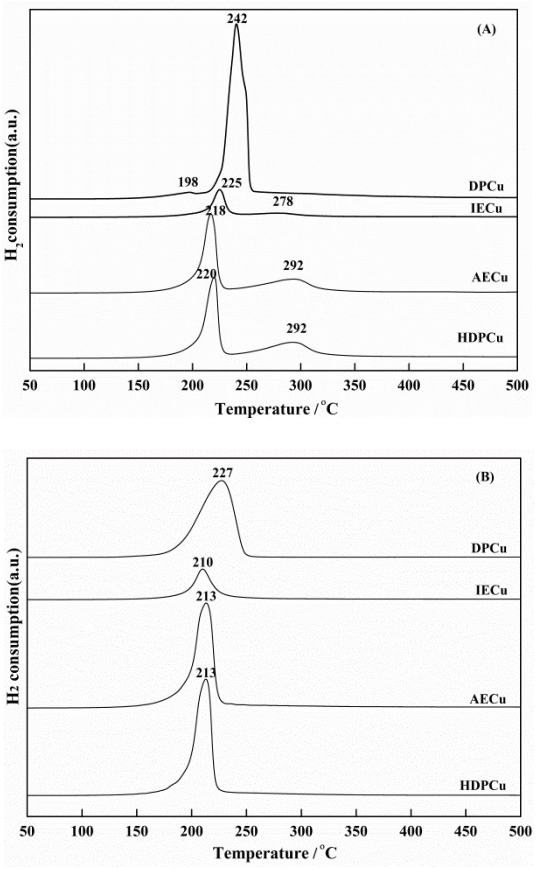

Fig. 4 TPR patterns of the Cu/SiO_2 samples. (A) dried, (B) calcined.

Catalytic Activity

Table 2 shows the catalytic performance of the Cu/SiO_2 catalysts for the hydrogenation of methyl acetate to ethanol. The main byproducts are methanol and ethyl acetate produced from the transesterification between the formed ethanol and the unconverted methyl acetate. The content of methanol was unchanged and the selectivity of ethyl acetate dropped at the expense of ethanol with the increase of MA conversion. The total content of the other byproducts including ethane, acetaldehyde, dimethyl ether and methyl ethyl ether was less than 2%. The data were collected with time on stream of 2 h. The activity of the four catalysts was in the order of AECu > HDPCu > IECu > DPCu. The Cu/SiO_2 catalyst prepared by the AE method showed the best performance for MA hydrogenation due to the high copper dispersion and surface area.

Discussion

Copper phyllosilicate, also called chrysocolla, is a kind of blue mineral copper silicate with a lamellar structure that consists of layers of SiO_4 tetrahedra sandwiched between discontinuous layers of CuO_6 octahedra.[21] Copper phyllosilicate was reported to form during the preparation of Cu/SiO_2 catalyst by the homogeneous deposition-precipitation method

Table 2 Reaction performance of the Cu/SiO_2 catalysts for the hydrogenation of methyl acetate

Catalyst	MA conversion (%)	Product selectivity (%)			
		Ethyl acetate	Methanol	EtOH	the others
DPCu	12.1	29.6	35.1	33.9	1.4
IECu	26.3	38.4	35.0	25.9	0.7
HDPCu	66.8	22.9	34.9	41.7	0.5
AECu	80.9	14.0	34.6	50.7	0.7

Reaction conditions: T = 220 °C, P = 1.0MPa, $n(H_2)/n(MA)$ = 40, and WHSV of MA = 1.0 h^{-1}.

using urea hydrolysis[9,22] and ion exchange of tetrammine copper cations onto the SiO_2 support.[4,23] Evaporation method is a kind of HDP method. Chen et al.[10] reported that copper phyllosilicate generated during the AE method, and it is supported by other researchers.[13-16] In the present work, the characterization results clearly show that copper phyllosilicate existed in the dried IECu, AECu and HDPCu samples and decomposed to CuO during the calcination at 450 °C. Upon calcination, the colour of the catalyst changed from blue, typical of an octahedral environment in chrysocolla, to olive green, characteristic of decomposed chrysocolla with a two-dimensional tenorite-on-silica structure.

The CuO in the calcined AECu did not exhibit black spot in the TEM image. By contrast, small CuO particles appeared in the calcined HDPCu and tended to agglomerate when exposure to the electron beam. The CuO in the two samples should come from different sources. Toupance[21,24] examined the conditions for the formation of copper phyllosilicate and confirmed that it was resulted from the reaction between silica acid arising from the dissolution of silica and $[Cu(OH)_2(H_2O)_4]^0$ complex in solution. According to Toupance's work, the optimal pH for the formation of copper phyllosilicate was ca. 9. Suitable pH value together with the water bath during the AE method resulted in fast dissolution of SiO_2 and enough $[Cu(OH)_2(H_2O)_4]^0$ complex. Therefore, we speculated that most of the copper species existed in the form of copper phyllosilicate in the dried AECu sample in the present work and the CuO in the calcined AECu came from the decomposition of copper phyllosilicate. This kind of CuO was in a high dispersion and stable under the electron beam due to the strong metal-support interaction. The small CuO particles which can merge into big particles in the calcined HDPCu were derived from $Cu(OH)_2$, which formed with the hydrolysis of urea and decomposed into CuO during the drying or calcination, rather than copper phyllosilicate. This type of CuO was sensitive to the electron beam due to the weak metal-support interaction. Therefore, two kinds of CuO from $Cu(OH)_2$ and copper phyllosilicate respectively coexisted in the calcined HDPCu. It was reported that three kinds of copper species existed in the dried IECu sample: copper phyllosilicate, isolated-grafted Cu^{2+} ions, and CuO from $Cu(OH)_2$.[21] Isolated-grafted Cu^{2+} came from the ion-exchange of $[Cu(NH_3)_4]^{2+}$ with hydroxyl groups on the silica surface. In general, the amount of isolated-grafted Cu^{2+} was less than 5% due to the limited amount of hydroxyl groups. For the IE method, the $Cu(OH)_2$ could not generate during the

ion-exchange procedure due to the high concentration of NH_3, but derived from the precipitation of the dissolved Cu^{2+} ions in the interstitial particle volumes during the washing procedure.[4] The disappearance of the large pores in the range of 10 nm to 28 nm during the AE and HDP methods indicated that the dissolution of the SiO_2 support was involved in the formation of copper phyllosilicate. Only few SiO_2 dissolved under room temperature in the IE method, so the yield of copper phyllosilicate was small and the Cu loading was only 7%.

In general, IE method resulted in high dispersion of the active sites. Herein, the catalyst prepared by the AE method possessed much higher copper loading than the IE catalyst, however it exhibited a better Cu^0 dispersion. Due to the formation of copper phyllosilicate in the catalyst precursor, the copper ions are homogeneously distributed over the silica support. The high copper dispersion in the reduced AE sample was caused by the high content of copper phyllosilicate in the catalyst precursor. For the IE and HDP methods, the existence of $Cu(OH)_2$ in the catalyst precursor lead to the lower copper dispersion than the AE method.

In some published papers[10,12,25] , the reduction of copper phyllosilicate was thought to cease at Cu^+, and further reduction of this kind of Cu^+ to Cu^0 was believed to require a high temperature of 600 ^oC due to the strong interaction between copper ions and SiO_2. As a result, the sole reduction peak of the calcined AECu and HDPCu samples in TPR was attributed to the collective reduction of copper phyllosilicate to Cu^+ and CuO to Cu^0 in these papers. Strangely, the reduction peak for Cu^+ was not observed although XPS/XAES gave a high Cu^+ content of more than 50% on the reduced catalyst sometimes. The premise of this point is that copper phyllosilicate still existed in the calcined samples. However, copper phyllosilicate have decomposed at 450 ^oC, the temperature which was adopted for the calcination. We did not exclude the possibility of some copper phyllosilicate existing in the calcined samples. According to Van Der Grift's report[20], chrysocolla did not exbibit H_2-consumption peak above 327 ^oC in TPR process. The in-situ XRD (Fig. 2D) showed that copper phyllosilicate in the dried AECu sample can be reduced to Cu^0 rather than Cu^+ below 350 ^oC. In addition, the reduction degree of the dried and calcined AECu was 95% and 99% respectively according to the TPR results. Therefore, even if some copper phyllosilicate were remaining in the calcined samples, they can be directly reduced to Cu^0 below 350 ^oC. Both CuO and copper phyllosilicate are reduced to Cu^0 based on the above results. However, as reported elsewhere, Cu^0 and Cu^+ coexisted in our reduced catalyst at 350 ^oC shown in our previous work.[26] In addition, Cu^+ widely existed in the chrysocolla-absent catalysts.[2,5,19]. In Zhu's work[5], the surface content of Cu^+ in the Cu/ZrO_2 and Cu/Al_2O_3 was about 50%. We thought that Cu^+ was ubiquitous in the reduced catalyst. Its formation may be related to the special surface topographies such as terrace, kink or edge. It is hard to attribute Cu^+ to some specific copper species.

Conclusions

Copper phyllosilicate generated during the preparation of Cu/SiO_2 catalyst by ion exchange, homogeneous deposition-precipitation assisted by the urea hydrolysis and ammonia evaporation method. CuO derived from the decomposition of copper phyllosilicate was stable due to the strong metal-support interaction and was reduced to highly dispersed copper particles. Copper phyllosilicate in the dried samples can be directly reduced to Cu^0 rather than Cu^+ without the calcination. The ammonia evaporation method was a suitable means to prepare the Cu/SiO_2 catalyst with high dispersion and high copper loading for ester hydrogenation due to the high content of copper phyllosilicate in the catalyst precursor.

Acknowledgements

This work was financially supported by National Nature Science Foundation of China (No. 21403215).

References

1 S. Wang, W. Guo, H. Wang, L. Zhu, S. Yin and K. Qiu, *New J. Chem.*, 2014, **38**, 2792-2800.
2 A. Yin, X. Guo, W. Dai, H. Li and K. Fan, *Appl. Catal. A*, 2008, **349**, 91-99.
3 M. Shimokawabe, N. Takezawa and H. Kobayashi, *Bull. Chem. Soc. Jpn.*, 1983, **56**, 1337-1340.
4 M. A. Kohler, H. E. Curry-Hyde, A. E. Hughes, B. A. Sexton and N. W. Cant, *J. Catal.*, 1987, **108**, 323-333.
5 Y. Zhu, Y. Zhu, G. Ding, S. Zhu, H. Zheng and Y. Li, *Appl. Catal. A*, 2013, **468**, 296-304.
6 Y. Zhu, X. Kong, D. Cao, J. Cui, Y. Zhu and Y. Li, *ACS Catal.*, 2014, **4**, 3675-3681.
7 D. S. Brands, E. K. Poels and A. Bliek, *Appl. Catal. A*, 1999, **184**, 279-289.
8 C. J. G. Vandergrift, P. A. Elberse, A. Mulder and J. W. Geus, *Appl. Catal.*, 1990, **59**, 275-289.
9 C. J. G. Vandergrift, A. F. H. Wielers, A. Mulder and J. W. Geus, *Thermochim. Acta.*, 1990, **171**, 95-113.
10 L. Chen, P. Guo, M. Qiao, S. Yan, H. Li, W. Shen, H. Xu and K. Fan, *J. Catal.*, 2008, **257**, 172-180.
11 A. Yin, X. Guo, W. Dai and K. Fan, *Catal. Commun.*, 2011, **12**, 412-416.
12 J. Gong, H. Yue, Y. Zhao, S. Zhao, L. Zhao, J. Lv, S. Wang and X. Ma, *J. Am. Chem. Soc.*, 2012, **134**, 13922-13925.
13 H. Yue, Y. Zhao, S. Zhao, B. Wang, X. Ma and J. Gong, *Nat. Commun.*, 2013, **4**, 2339-2346.
14 H. Yue, Y. Zhao, X. Ma and J. Gong, *Chem. Soc. Rev.*, 2012, **41**, 4218-4244.
15 H. Yue, X. Ma and J. Gong, *Acc. Chem. Res.*, 2014, **47**, 1483-1492.
16 F. Li, C. Lu and X. Li, *Chin. Chem. Lett.*, 2014, **25**, 1461-1465.
17 H. Lin, X. Zheng, Z. He, J. Zheng, X. Duan and Y. Yuan, *Appl. Catal. A*, 2012, **445**, 287-296.
18 X. Zheng, H. Lin, J. Zheng, X. Duan and Y. Yuan, *ACS Catal.*, 2013, **3**, 2738-2749.
19 A. Yin, X. Guo, W. Dai and K. Fan, *J. Phys. Chem. C*, 2009, **113**, 11003-11013.
20 C. J. G. Vandergrift, A. Mulder and J. W. Geus, *Appl. Catal.*, 1990, **60**, 181-192.
21 T. Toupance, M. Kermarec, J. F. Lambert and C. Louis, *J. Phys. Chem. B*, 2002, **106**, 2277-2286.

22 S. Wang, X. Li, Q. Yin, L. Zhu and Z. Luo, *Catal. Commun.*, 2011, **12**, 1246-1250.
23 M. Shimokawabe, N. Takezawa and H. Kobayashi, *Appl. Catal.*, 1982, **2**, 379-387.
24 T. Toupance, M. Kermare and C. Louis, *J. Phys. Chem. B*, 2000, **104**, 965-972.
25 S. Zhu, X. Gao, Y. Zhu, W. Fan, J. Wang and Y. Li, *Catal. Sci. Technol.*, 2015, **5**, 1169-1180.
26 X. Ma, Z. Yang, X. Liu, X. Tan and Q. Ge, *RSC Adv.*, 2015, **5**, 37581-37584.

Table of contents entry

Copper phyllosilicate turned into Cu^0 rather than Cu^+ after calcination and reduction.